

KEYWORDS: Monte Carlo code, reactor simulation, activation measurement

MONTE CARLO MODELING OF THE PORTUGUESE RESEARCH REACTOR CORE AND COMPARISON WITH EXPERIMENTAL MEASUREMENTS

ANA C. FERNANDES,* ISABEL C. GONÇALVES, NUNO P. BARRADAS,
and ANTÓNIO J. RAMALHO Nuclear and Technological Institute
Estrada Nacional 10, 2686-953 Sacavém, Portugal

Received May 7, 2002

Accepted for Publication December 18, 2002

The Monte Carlo code MCNP-4C was used to calculate the effective multiplication coefficient of a core configuration of the Portuguese Research Reactor (RPI) and the neutron fluxes in the core and in the reflector region.

A comparison of the results obtained with MCNP and with the deterministic codes WIMSD-5 and CITATION was made. Consistent deviations of 2% for the effective multiplication constant and 8 to 28% for the neutron flux, depending on the energy range, were observed.

Thermal, epithermal, and fast neutron flux measurements were performed using activation detectors. The calculations agree with experimental values within <15%; therefore, the Monte Carlo results can be used to predict the neutron field in other locations and irradiation facilities of the RPI.

I. INTRODUCTION

The Portuguese Research Reactor (RPI) is a 1-MW swimming pool-type reactor located in the campus of the Nuclear and Technological Institute, and it has been operating since 1961. The expansion of activities into which the RPI is being involved requires improvements both in calculation and experimental methods for studying the radiation field in the irradiation facilities.

The neutron field at half-height of the RPI core is routinely calculated with the standard two-dimensional computer codes WIMSD-5 (Ref. 1) and CITATION (Ref. 2), using a homogenizing procedure to describe the fuel elements and considering four energy groups.³

The significant decrease in computational costs and the enhanced sophistication of codes have motivated a widespread use of Monte Carlo radiation transport simulation in recent

years.⁴ In particular, regulatory agencies are encouraging the use of Monte Carlo methods for *decision-making* in health physics and nuclear safety areas because of the potential for very precise geometrical models and the use of continuous-energy data.

A detailed three-dimensional continuous-energy Monte Carlo model of RPI was developed using the MCNP-4C code.⁵ The model was used to calculate the effective multiplication constant k_{eff} and the neutron field in several locations in the reactor core and reflector. The results obtained from both calculation methods were compared. The MCNP model was validated through measurements with activation detectors.⁶ Vertical detector response profiles were determined with the detectors placed in the water channels between the fuel plates and at several positions of the core grid plate. A polynomial fit to the measurements yields an average detector response suitable for comparison with the calculations.

II. CORE DESCRIPTION

The reactor core is an assembly of fuel elements mounted on a grid plate with a 9×6 pattern (Fig. 1). It is reflected by a graphite thermal column in one side, beryllium on two sides, and light water on the other side. A partial aluminum reflector is used to enhance the fast neutron flux in one beam tube. The fuel is material test reactor (MTR)-type, flat plates, using 93.2% enriched uranium. The fuel plates are aluminum clad, and the meat is a U-Al alloy containing 14.72 ± 0.08 g of ^{235}U (1σ) (Ref. 7). The active length of the fuel elements is 60 cm, and the cross section is approximately square with an 8-cm side length. The density of the fresh fuel meat is 3.21 g cm^{-3} , and the moderator temperature is $<40^\circ\text{C}$.

There are two types of fuel elements, standard (Fig. 2a) and control (Fig. 2b). The standard fuel elements have 18 plates each, and the control elements have 10 fuel plates and 2 inner dummy aluminum plates. For identification purposes, the spaces between the fuel plates are numbered according to their proximity to the thermal column.

There are four safety rods and one regulating rod located in the control elements. The regulating rod is a massive stainless

*E-mail: anafer@itn.pt

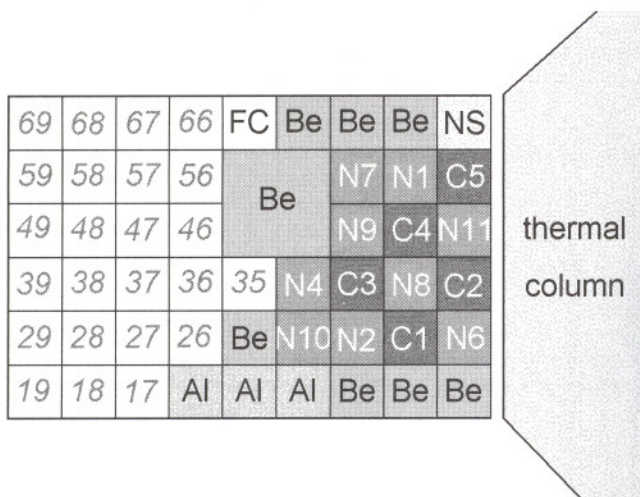


Fig. 1. The N2-P1/6 configuration of the RPI. (Be = beryllium reflector; Al = aluminum reflector; C = control fuel element; N = standard fuel element; FC = fission chamber; NS = neutron source). The grid positions are labeled in *italic*. Measurements were done in fuel elements N7, N4, and N10 and in the irradiation positions 35, 36, 26, 56, and 17.

steel bar, while the safety rod consists of a 1-mm-thick cadmium foil wrapped around a stainless steel tube and covered by stainless steel.

III. MCNP MODEL

The Los Alamos National Laboratory MCNP-4C code is a general-purpose Monte Carlo code that can numerically simulate neutron, photon, and electron transport. The input to MCNP includes a geometrical description of the system to be modeled, the neutron source, cross-section tables, the parameters to be tallied, and miscellaneous data such as running options or cutoff criteria. When calculating k_{eff} , the distribution of source points in the fissile material is iteratively determined

by the code and should converge from an initial arbitrary distribution.

The RPI model for MCNP was based on an accurate material and geometrical database obtained from the technical specification sheet. Fuel burnup and composition were calculated with WIMSD/CITATION. The cell-homogenized group constants are calculated with WIMSD in the thermal ($E < 625$ meV), resolved resonances ($625 \text{ meV} < E < 5.53 \text{ keV}$), unresolved resonances ($5.53 \text{ keV} < E < 821 \text{ keV}$), and fast ($821 \text{ keV} < E < 10 \text{ MeV}$) energy regions. These group constants are iteratively used in the CITATION calculations of power density and changes in fuel composition during a time step. For the standard fuel assembly, one homogenized region composed of the 18 fuel plates and surrounding water is considered, whereas the control assembly is described using two separate fuel regions, as shown in Fig. 2. Each homogenized fuel region is assumed to have a uniform burnup and composition. From the results obtained for the two regions of the control assemblies, this assumption is accurate within 0.5% in the central core region and 3% in the periphery. The configuration of the RPI core studied included fuel with burnup as much as 25%. The cross-section library used for the MCNP calculations was ENDF-B/VI. Thermal neutron scattering by molecules and solids was included for graphite, hydrogen in water, and beryllium. A constant temperature of 300 K was considered for all the materials.

The geometrical model (Fig. 3) included the detailed structure of the fuel elements so as to take advantage of the MCNP ability to deal with complex geometries. The core arrangement was achieved by defining a priori the various elements (i.e., a standard and a control fuel element, a control rod, a beryllium and an aluminum reflector) and distributing them throughout the core grid in the pattern of the configuration to be studied.

IV. CALCULATIONS

An initial source distribution with one point in each fuel element and an arbitrarily assumed value of $k_{eff} = 1$ were used for running typically 2000 cycles of 5000 particles each. A good settling was achieved with 5 cycles. The running time for 1 million particles was in the order of 400 min on a Pentium III 1-GHz personal computer.

The detection regions for tallying the neutron flux were considered as cylinders, 10 cm in length and 0.3 cm diameter, centered at the midheight of the fuel. The average neutron flux in the detector volume was calculated for the energy group structure used in WIMS/CITATION. Occasionally, the 47 energy groups of the BUGLE-80 structure⁸ were also considered. Figure 4 shows the calculated neutron energy spectrum at grid position 35. The figure also shows the thermal (Maxwell at 293.15 K), epithermal 1/E, and Watt-Cranberg distributions, after normalization to the neutron flux in the thermal, resolved resonances, and fast energy regions. The first energy group of the BUGLE structure was split to show more clearly the adjustment in the thermal energy region.

The responses (i.e., the saturation activity per target atom) of the activation detectors for the reactions considered in the measurements (Table I) were calculated using the continuous-energy activation cross sections of the LLLDOS library.

A comparison between MCNP and WIMSD calculations was made for several reactor parameters, namely, the k_{eff}

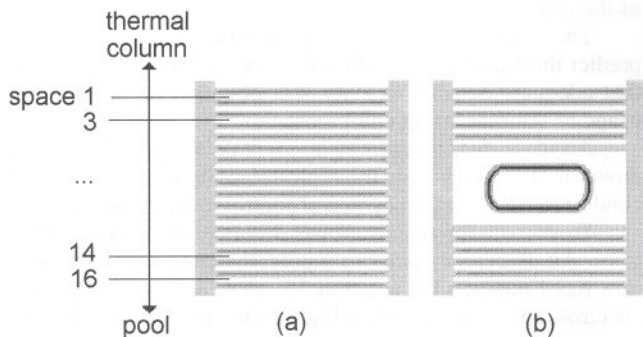


Fig. 2. Cross section of the (a) standard and (b) control fuel elements (including a safety rod) and labeling of spaces between the fuel elements.

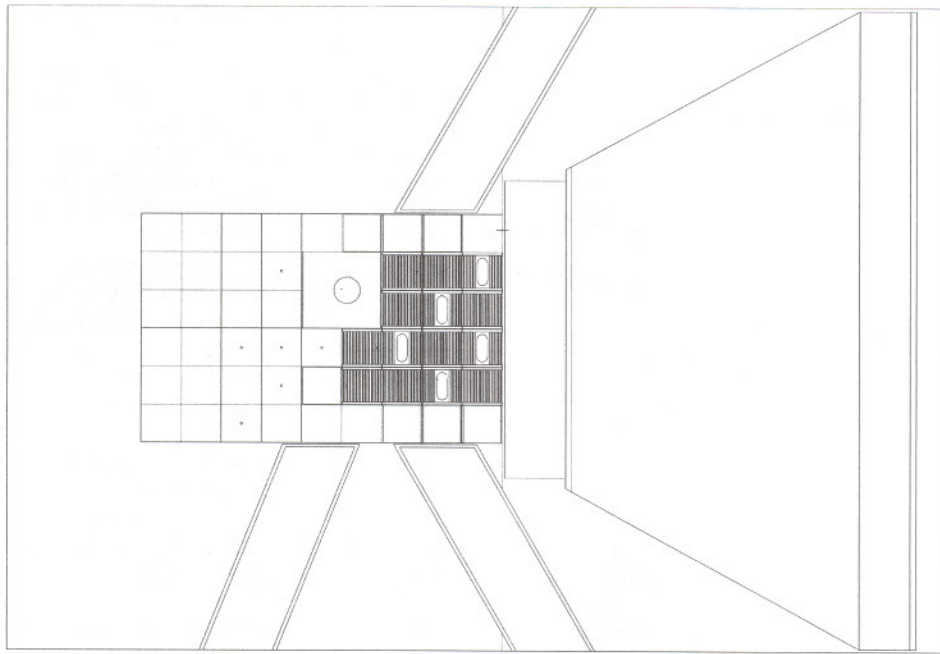


Fig. 3. Cut view of the modeled configuration. Some detection volumes for tallying the neutron flux are also shown.

(Table II) and the neutron flux in the positions evaluated in this work (Fig. 5). The uncertainties presented in the MCNP values are solely because of the statistical nature of the code. These are in the order of 1% (1σ) for the thermal, 2% for the resolved resonances, 3% for the unresolved resonances, and 3% for the fast energy regions.

The differences between the neutron fluxes calculated with MCNP and WIMSD are $(11.2 \pm 0.8)\%$, $(28 \pm 2)\%$, $(8.2 \pm 0.8)\%$, and $(17 \pm 1)\%$, respectively, for thermal, resolved resonances, unresolved resonances, and fast energy regions. These

differences are still significant, and further work will be performed to clarify the situation.

V. MEASUREMENTS

Activation foil measurements were performed in the interplate spaces of the fuel elements and in some irradiation positions of the core support grid plate (Fig. 1) to determine the vertical neutron flux profile. The foils were placed in aluminum (for the in-core measurements) and polyethylene (for measurements in the irradiation positions) supports, distributed in such a way as to cover the full length of the active core.

The activation detectors and reactions considered are listed in Table I (Ref. 9). The Mn and Au foils were used for thermal and epithermal neutron detection; In, Ni, and Al wrapped in 0.5-mm cadmium were used for measuring the fast component of the neutron spectrum.

The calculated values of the neutron flux were used to predict the irradiation conditions (time and reactor power) so that adequate detector activity was obtained for the optimal usage of the measuring equipment.

All the in-fuel measurements were performed after a shutdown of at least 48 h, as the reproducibility of the irradiation conditions (namely, the position of control rods) is best achieved.

To correct for reactor power fluctuation among irradiations, Au detectors placed in a polyethylene support inserted in a fixed position (at position 35) were used. A gamma-ray spectroscopy system with a high-purity germanium detector was used for the activity measurements.

The vertical profiles of detector responses were determined for the various irradiation positions. Figure 6 shows the measured and calculated vertical profile obtained for Au foils

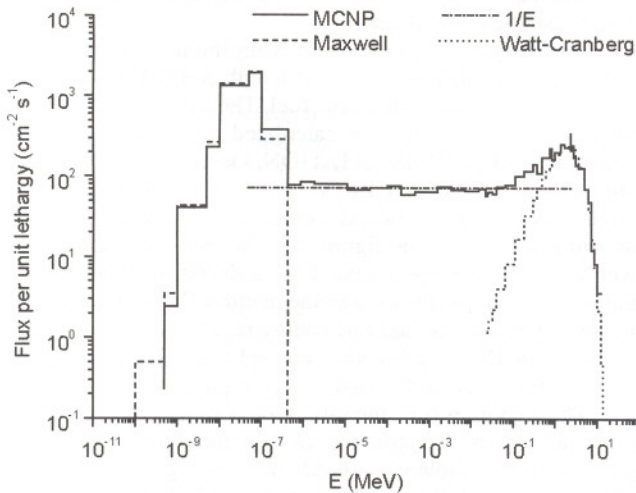


Fig. 4. Calculated neutron energy spectrum in position 35 and adjusted Maxwell, epithermal 1/E, and Watt-Cranberg shapes.

TABLE I
Activation Detectors and Reactions Used for the Measurements at RPI

Reaction	Detector	Cross Section ^a	T _{1/2}	90% Response in MTR Spectrum
⁵⁵ Mn(n, γ) ⁵⁶ Mn	Mn-Al 0.1% w/w ^b (0.1 × diameter 5) mm	σ ₀ = 13.3 (2) b I ₀ = 14.0 (3) b	2.577 (1) h	5.5 meV to 340 eV
¹⁹⁷ Au(n, γ) ¹⁹⁸ Au	Au-Al 0.1% w/w (0.1 × diameter 5) mm	σ ₀ = 98.65 (9) b I ₀ = 1550 (28) b	2.696 (2) days	15 meV to 5.8 eV
¹¹⁵ In(n, n') ^{115m} In	(0.127 × diameter 10) mm	σ _{fis} = 122 (21) mb	4.486 (4) h	1.0 to 5.6 MeV
⁵⁸ Ni(n, p) ⁵⁸ Co	(0.05 × diameter 10) mm	σ _{fis} = 102.3 (67) mb	70.82 (3) days	1.9 to 7.5 MeV
²⁷ Al(n, α) ²⁴ Na	(0.127 × diameter 10) mm	σ _{fis} = 0.685 (37) mb	14.959 (4) h	6.5 to 12 MeV

^aIn the cross-section column, I₀, σ₀, and σ_{fis} are, respectively, the resonance integral and the thermal and fission equivalent (in ²³⁵U fission spectrum) cross sections.

^bw/w = weight fraction.

irradiated in position 35. The different vertical profiles result from a distortion caused by the insertion of the control rods, as most of the fission reactions occur in the lower region of the fuel.

For comparison with calculations, the experimental detector responses were determined at midheight of the fuel elements, after polynomial fittings to the measured profiles.

The most important contributions to the overall uncertainty are the activity measurements (2% mainly from detector calibration), polynomial adjustment (1%), and monitoring of irradiation conditions (2%), from which a total value of 6% was estimated.

The calculated saturation activity for the reactions indicated in Table I, at midheight of the fuel elements, and the ratio of calculated-to-experimental values are shown in Tables III and IV. The results were obtained with a 70 million particle run and were normalized to the measured response of gold foils in position 35 at midheight of the fuel elements (A_{sat} = 2.57 × 10⁻⁹ s⁻¹ atom⁻¹).

An agreement better than 15% was found for all cases, even for the Al detectors placed in locations outside the reactor

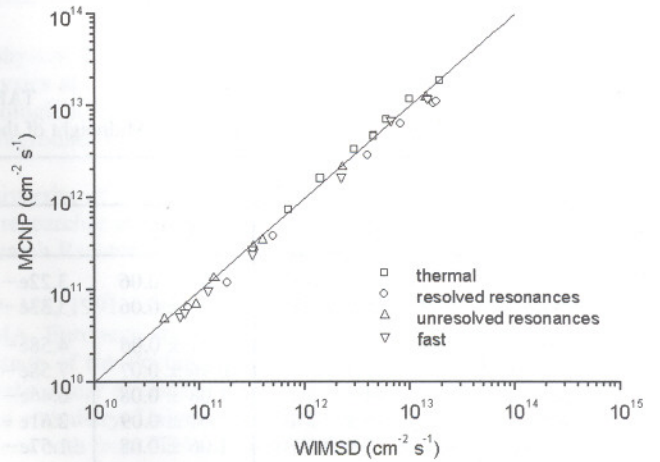


Fig. 5. Neutron flux calculated with WIMS and MCNP in four energy regions. The results were normalized to the thermal neutron flux in position 35. The solid line corresponds to a 1:1 relation between the calculations.

TABLE II
Core Effective Multiplication Constant *k_{eff}* and Reactivity Worth of Some Control Rods and Reflectors, Calculated with MCNP and WIMS*

	MCNP	WIMS
<i>k_{eff}</i> with		
Fresh fuel		
Rods in	0.96633 ± 0.00026	0.95681
Rods out	1.11572 ± 0.00025	1.09537
Burned fuel		
Rods in	0.89113 ± 0.00026	0.87879
Rods out	1.03063 ± 0.00025	1.00937
Reactivity worth of		
Rod S1	0.02519 ± 0.00025	0.02436
Rod R5	0.00391 ± 0.00025	0.00362
Al reflector	0.00284 ± 0.00024	0.0032

*Reactivity worths are determined by comparing *k_{eff}* with and without the rod or reflector. The uncertainties correspond to 1σ.

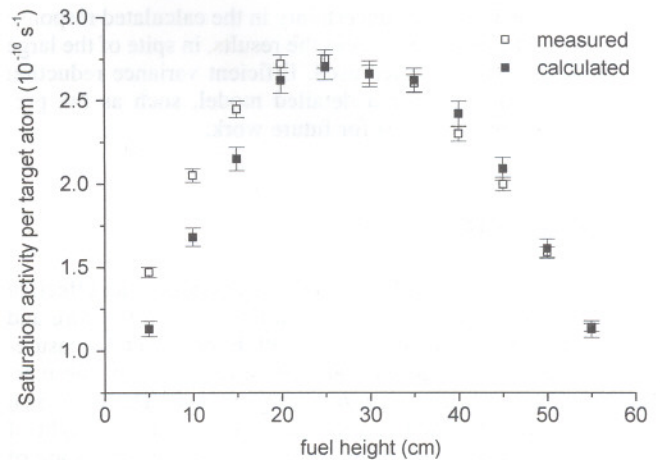


Fig. 6. Measured and calculated vertical profile of Mn detectors response in grid position 35. The origin of the x axis corresponds to the bottom of the fuel. The calculated values were normalized to the measurement at half-height of the fuel.

TABLE III
Calculated Responses at Midheight of the Fuel Elements for Thermal and Epithermal Neutron Detectors*

Irradiation Position	Mn		Au	
	C	C/E	C	C/E
N10, space 16	$9.29\text{e}-11 \pm 0.84\%^a$	1.11 ± 0.07	$1.85\text{e}-9 \pm 2.0\%$	0.94 ± 0.06
N4, space 2	$1.53\text{e}-10 \pm 0.68\%$	1.10 ± 0.07	$3.18\text{e}-9 \pm 1.6\%$	1.07 ± 0.07
N7, space 2	$1.54\text{e}-10 \pm 0.68\%$	1.05 ± 0.07	$3.08\text{e}-9 \pm 1.6\%$	0.94 ± 0.06
Position 35	$2.62\text{e}-10 \pm 0.48\%$	1.03 ± 0.06	$2.57\text{e}-9 \pm 0.86\%$	1.00 ± 0.06
Position 36	$6.60\text{e}-11 \pm 0.87\%$	0.89 ± 0.04	$5.84\text{e}-10 \pm 1.6\%$	0.90 ± 0.05
Position 26	$6.47\text{e}-11 \pm 0.90\%$	0.97 ± 0.06	$5.95\text{e}-10 \pm 1.6\%$	0.98 ± 0.06
Position 56	$4.69\text{e}-11 \pm 1.0\%$	0.93 ± 0.05	$3.92\text{e}-10 \pm 1.6\%$	0.92 ± 0.05
Position 17	$2.23\text{e}-11 \pm 1.5\%$	1.01 ± 0.06	$1.95\text{e}-10 \pm 2.5\%$	1.00 ± 0.06

*C: calculated responses. The deviation from experimental measurements E is indicated by the ratio C/E. The calculated values were normalized to the saturation activity of the gold foils at position 35.

^aRead as $9.29 \times 10^{-11} \pm 0.84\%$.

TABLE IV
Calculated Responses at Midheight of the Fuel Elements for Fast Neutron Detectors*

Irradiation Position	Ni		In		Al	
	C	C/E	C	C/E	C	C/E
N4, space 2	$8.76\text{e}-13 \pm 1.0\%^a$	0.94 ± 0.06	$3.22\text{e}-12 \pm 0.67\%$	1.04 ± 0.04	$1.10\text{e}-14 \pm 5.1\%$	0.90 ± 0.05
N7, space 2	$9.25\text{e}-13 \pm 1.0\%$	1.07 ± 0.06	$3.33\text{e}-12 \pm 0.66\%$	1.05 ± 0.06	$1.31\text{e}-14 \pm 4.6\%$	1.06 ± 0.08
Position 35	$1.30\text{e}-13 \pm 1.9\%$	0.91 ± 0.06	$4.58\text{e}-13 \pm 1.3\%$	0.90 ± 0.05	$2.77\text{e}-15 \pm 8.1\%$	0.97 ± 0.10
Position 36	$2.30\text{e}-14 \pm 4.4\%$	0.96 ± 0.07	$7.58\text{e}-14 \pm 3.0\%$	0.95 ± 0.06	$5.22\text{e}-16 \pm 20\%$	1.10 ± 0.23
Position 26	$1.97\text{e}-14 \pm 4.8\%$	1.08 ± 0.08	$6.46\text{e}-14 \pm 3.2\%$	0.93 ± 0.06	$4.32\text{e}-16 \pm 18\%$	1.11 ± 0.24
Position 56	$8.45\text{e}-15 \pm 7.2\%$	1.01 ± 0.09	$2.61\text{e}-14 \pm 4.8\%$	1.09 ± 0.08	$8.36\text{e}-17 \pm 25\%$	0.86 ± 0.22
Position 17	$4.75\text{e}-15 \pm 9.5\%$	1.06 ± 0.08	$1.57\text{e}-14 \pm 6.5\%$	0.94 ± 0.09	$1.10\text{e}-16 \pm 38\%$	0.94 ± 0.35

*C: calculated responses. The deviation from experimental measurements E is indicated by the ratio C/E. The calculated values were normalized to the saturation activity of the gold foils at position 35.

^aRead as $8.76 \times 10^{-13} \pm 1.0\%$.

core, for which the high uncertainty in the calculated response was due to the poor statistics in the results, in spite of the large number of particle stories used. Efficient variance reduction techniques adequate for a detailed model, such as the presented one, are of interest for future work.

VI. CONCLUSIONS

The MCNP-4C code was used to determine the effective multiplication constant and neutron flux both in the core and in the grid irradiation positions of RPI. Experimental measurements were performed with activation detectors for the thermal, epithermal, and fast neutron energy regions. The agreement between the calculated and measured values at midheight of the fuel elements was within 15%. These discrepancies are of the same order as obtained in similar investigations, using coupled MCNP and burnup calculations.¹⁰ The model was therefore validated with experimental measurements. The model presented is able to simulate the neutron field close to the

reactor core and can be used to obtain the source for subsequent calculations of the radiation field in other irradiation facilities of RPI.

ACKNOWLEDGMENTS

The authors wish to express their gratitude to J. Santos for the technical support and to the operation group of RPI for the careful positioning of the detectors. A. C. Fernandes acknowledges the Foundation for Science and Technology for a PhD grant.

REFERENCES

1. "WIMSD—A Neutronics Code for Standard Lattice Physics Analysis," NEA 1507/02, Nuclear Energy Agency (June 1997).
2. "CITATION Tape Description and Implementation Information," NESC 387.360K Note 81-66, National Energy Software Center (1981).

3. N. P. BARRADAS, F. CARDEIRA, A. C. FERNANDES, I. C. GONÇALVES, J. G. MARQUES, and A. J. G. RAMALHO, "Neutronics Study of Core 2 of the Portuguese Research Reactor," ITN/RPI-R-00/57, Nuclear and Technological Institute (2000).
4. *Proc. Int. Conf. Advanced Monte Carlo for Radiation Physics, Particle Transport Simulation and Applications*, Lisbon, Portugal, October 23–26, 2000, A. KLING, F. BARÃO, M. NAKAGAWA, L. TÁVORA, and P. VAZ, Eds., Springer-Verlag, Berlin (2001).
5. J. BRIESMEISTER, "MCNP—A General Monte Carlo N-Particle Transport Code System, Version 4C," LA-13709-M, Los Alamos National Laboratory (2000).
6. "Neutron Fluence Measurements," IAEA Technical Report Series 107, International Atomic Energy Agency (1970).
7. "Core Physics and Shielding—RPI Portuguese Research Reactor," ER 7429, ER 7503, AMF Atomic (1959).
8. R. W. ROUSSIN, "BUGLE-80 Coupled 47-Neutron, 20-Gamma-Ray P3 Cross Section Library," DLC-75, Radiation Shielding Information Center, Oak Ridge National Laboratory (1980).
9. J. H. BAARD, W. L. ZIJP, and H. J. NOLTHENIUS, *Nuclear Data Guide for Reactor Neutron Metrology*, Kluwer Academic Publishers, The Netherlands (1989).
10. R. NABBI and J. WOLTERS, "Application of MCNP4B for Criticality Analysis of FRJ-2," *Proc. 4th Int. Topl. Mig. Research Reactor Fuel Management*, Colmar, France, March 19–21, 2000, p. 37, European Nuclear Society (2000).

Ana C. Fernandes (BS, engineering physics, Technical University of Lisbon, Portugal, 1997) is a PhD student in nuclear physics at the University of Lisbon. The thesis work is developed at the Nuclear and Technological Institute (ITN) in the area of mixed-field dosimetry for nuclear reactors. Her background includes thermoluminescent dosimetry and Monte Carlo simulation.

Isabel C. Gonçalves (BS, physics, University of Lisbon, Portugal, 1964; Graduate Researcher, ITN, Portugal, 1980) is senior researcher at the ITN. She is responsible for the dosimetry group of the Portuguese Research Reactor. Her background includes neutron spectrometry and reactor dosimetry.

Nuno P. Barradas (BS, physics, 1989; MS, 1991, and PhD, 1994, applied nuclear physics, University of Lisbon, Portugal; MA, European studies, University of Surrey, 1999) is responsible for the calculations group of the Portuguese Research Reactor at ITN. His background includes computational nuclear physics and ion beam analysis.

António J. Ramalho (BS, physics and chemistry, University of Lisbon, Portugal, 1954; Genie Atomique, Saclay, 1957) is retired both from ITN and from the International Atomic Energy Agency. His background includes research reactor operation and exploitation and safeguards experiments, especially nondestructive assay measurements on all the materials for a nuclear cycle.